Large Eddy Simulation of a LOx/CH_4 swirl flame under transcritical conditions

M. Bouton[a,b], A. Nicole[c], A. Genot[d], G. Ribert[e]
[a]DMPE, ONERA, Université Paris Saclay, 91120, Palaiseau, France
[b]CNES - Transport spatial - Etablissement de Daumesnil, F-75612 Paris Cedex, France
[c]DTIS, ONERA, 13330, Salon-de-Provence, France
[d]DMPE, ONERA, Université de Toulouse, 31000, Toulouse, France
[e]CORIA - CNRS, Normandie Université, INSA Rouen Normandie, Rouen, 76000, France

1 Introduction

To enhance the performance of Liquid Rocket Engine (LREs) operating at high pressure, swirl-type injection is a promising approach. Swirl injection promotes mixing of reactants, better flame stabilization, and higher combustion efficiency [1]. However, similar to coaxial injectors, the stability of flame dynamics remains a key criterion in LRE development. A deeper understanding of high-pressure swirl flames is therefore essential for optimizing the design of swirl-type injectors.

With the increasing capabilities of numerical simulations, computational tools have become essential for studying rocket engine-type flows [2] since experimental investigations are often constrained by the extreme pressure and temperature conditions typical of LREs [2, 3]. In particular, the development of suitable numerical models is crucial for accurately capturing the flow structure. This study focuses on a configuration recently examined within a joint ONERA/CNES research program [3] using the MASCOTTE test bench. The setup involves a transcritical swirl injection of liquid oxygen (LOx) surrounded by a high-pressure methane co-flow, operated without acoustic forcing. Despite its increasing relevance in space propulsion applications, the LOx/CH_4 transcritical swirl flame remains relatively underexplored. Previous studies have examined similar configurations, including cold-flow LOx swirl injectors [4, 5], bi-swirl LOx/kerosene flames [6] and multi-injector LOx/CH_4 swirl flames [7]. These works underline the need for further research to fully understand the flame dynamics of LOx/CH_4 systems.

In this work, we aim to contribute to the understanding of these complex flows. Simulations are performed using ONERA flow solver CEDRE, and the numerical results are first validated against experimental data [3], before conducting an in-depth analysis of the flow behavior.

2 Numerical configuration

CEDRE Computational Fluid Dynamics platform from ONERA deals with the complex flow encountered in the field of energetics and propulsion, considering various physical and chemical phenomena

Correspondence to: maxime.bouton@onera.fr

and the associated coupling mechanisms. CEDRE uses a multi-physics approach based on the coupling of specialized solvers on general unstructured meshes, which allows great flexibility in considering the most technological effects [8]. It has already been used successfully for the simulation of transcritical LOx/CH_4 flames [9, 10].

The numerical domain is the entire MASCOTTE *Bhp-Hrm* combustion chamber [11]. The geometry is given in Fig. 1a. Several meshes were generated to perform mesh convergence. The reference mesh contains 5 millions elements. Additional informations and justifications will be provided to describe mesh dependence. Smallest cell size is $6.10^{-5}m$ and lip thickness separating the LOx and methane streams is discretized by about 7 cells. As illustrated in Fig. 1b, LOx and methane are injected at a transcritical and supercritical state, respectively, with a mixture ratio of 4.3 into a pressure environment of 62 bar, close to a chamber operating point. To reproduce experimental conditions [3], helium is also injected at the injection plane and in the nozzle to simulate cooling of the visualization windows and nozzle wall. Injectors walls are set as no-slip boundary conditions with imposed temperatures equal to the injection temperatures of the incoming fluids. No-slip and adiabatic boundary conditions are applied to the chamber walls. Two different wall laws are used [12]. One is adapted to a channel flow and is based on the Reynolds which depends on the velocity in the wall-cell. The second one is adapted to detached flows and is based on the turbulent Reynolds. They are used for the injectors and combustor walls, respectively. Non-reflecting boundary conditions are applied to the inlets and outlet [13], allowing acoustic energy to exit. The convective fluxes at the mesh faces are determined by the HLLC method [14]. Time is advanced with an implicit linear system using a GMRES method [15].

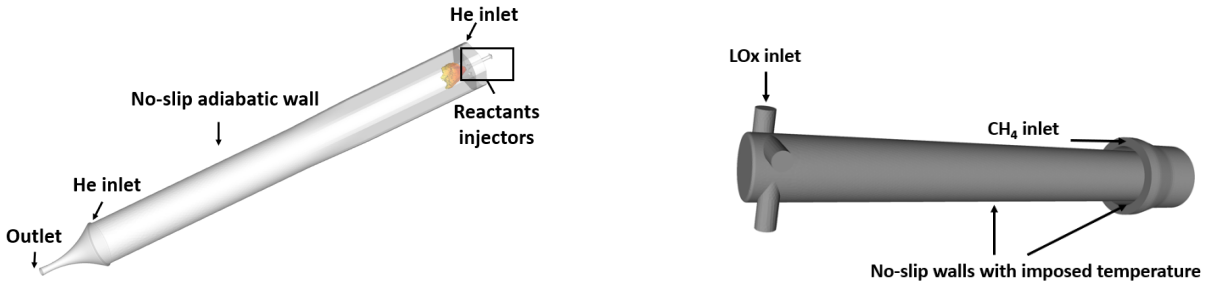

(a) Computational domain geometry.

(b) Reactants injectors geometry.

Figure 1: Left: Computational domain geometry. Right: Reactants injectors geometry.

Currently, no consensus exists on the optimal subgrid-scale model for representing turbulence in such configurations [16], although the Smagorinsky model remains the most commonly adopted [4, 6, 7]. LES is performed with this last subgrid-scale model with the constant $C_s = 0.15$. As it is commonly used in high-pressure LRE previous simulations [17], combustion is here described with an infinitely fast chemistry model. A relaxation towards the local thermodynamic equilibrium state for a given set of species $\{O_2; CH_4; CO_2; H_2O; OH; H_2; CO; H; O\}$ is used [18]. The selected species for the simulation correspond to the major species identified from an equilibrium computation performed using Cantera. Maximum local relaxation characteristic time is limited to 40 time steps (for robustness reasons [17]). This approach provides a more accurate flame temperature than the EBU model [18]. Regarding thermodynamic, a two-fluid approach is used with the compressed liquid (or dense) phase, i.e. LOx, and CH_4 modeled by a Soave-Redlich-Kwong equation of state (as in [17, 19]) and Ely-Hanley model [20] for transport properties. An ideal gas description is used for combustion products and gaseous O_2.

Finally, as LOx is injected under transcritical conditions into an environment where the temperature exceeds its critical point, it shifts to a supercritical state. A pseudo-vaporization model [21] is used to simulate the pseudo-chemical reaction: $O_{2,liquid} \longleftrightarrow O_{2,supercritical}$. Chemical conversion is governed

by a relaxation towards an equilibrium model whose characteristic relaxation time is of the order of the time step.

3 Results and validations

All these models are implemented and compared with experimental data [3] in order to assess their accuracy and predictive capabilities on flame structure and dynamics. In Fig. 2, several contours (black dots) from line-of-sight time-averaged integrated density and heat release rate are respectively compared with the time-averaged backlighting and OH* chemiluminescence fields. The black spots correspond to different percentages of the integrated density and heat release rate maximum values. Comparisons between experimental and numerical fields is still to be discussed. Dense core opening angle and length compared with backlighting data are encouraging. Comparisons between the heat release rate and OH* chemiluminescence is more challenging. Moreover, it was suggested by Fiala et al. [22] that under high temperature and pressure conditions, OH radical excitation is primarily driven by thermal processes rather than chemical reactions and that OH* concentration exponentially depends on temperature.

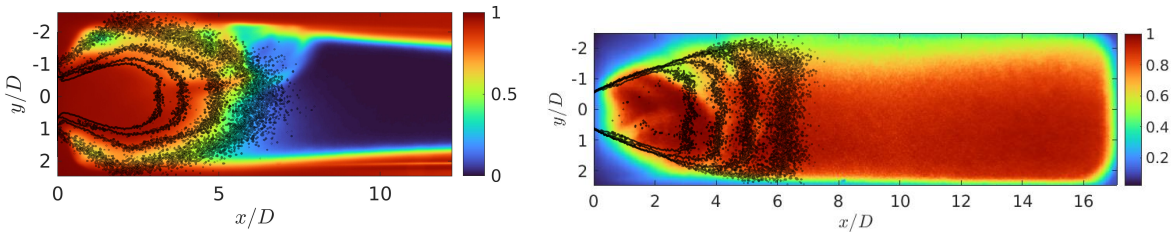

(a) Experimental time-averaged backlighting field [3] compared with line-of-sight time-averaged integrated density contours (black dots). Blue: light phase. Red: Dense phase.

(b) Experimental time-averaged OH* chemiluminescence field [3] compared with line-of-sight time-averaged integrated heat release rate contours (black dots). Blue: no OH* emission. Red: OH* emission.

Figure 2: Comparisons between time-averaged experimental analysis fields [3] and numerical contours

Then, simulation allows to go further in the flow analysis. Fig. 3 illustrates the instantaneous flowfields. In Fig. 3a, a region of negative axial velocity (dark blue) is observed downstream of the injector exit ($x/R > 0$), indicating the development of a reverse flow that extends upstream into the swirler ($x/R < 0$). This reverse flow forms a gaseous core composed of the light phase originating from the combustor, as shown by the density stratification within the swirler in Fig. 3b. Because of the swirl motion, a film of dense fluid (LOx) forms along the injector wall and propagates downstream. Small-amplitude waves, resulting from hydrodynamic instabilities [6], are observed at the interface between the light and dense phases within the swirler ($y/R \pm 0.9$). At the injector exit, transcritical LOx is heated and evaporates into supercritical oxygen. Fig. 3c shows that oxygen and methane mix and burn in the recess region at the lip separating the two injectors. Further downstream, the flame front is wrinkled by shear layer instabilities and turbulence [6]. Spectral analysis through Fast Fourier Transform will be made to compared jet dynamics with Bouton et al. [3].

To further understand the flow dynamics of the LOx injector, radial distributions are extracted from the 20 ms time-averaged fields, along the red LOx tube radius at $x/R = -4$ of Fig. 3a. Distributions of the quantities are non-uniform along the injector radius and are given in Fig.4. Fig. 4a shows that the axial velocity becomes negative at $y/R = 0.5$ because of the central recirculation zone downstream of the injector. As illustrated in Fig. 4b and Fig. 4c, the rotational motion is more intense in the dense phase

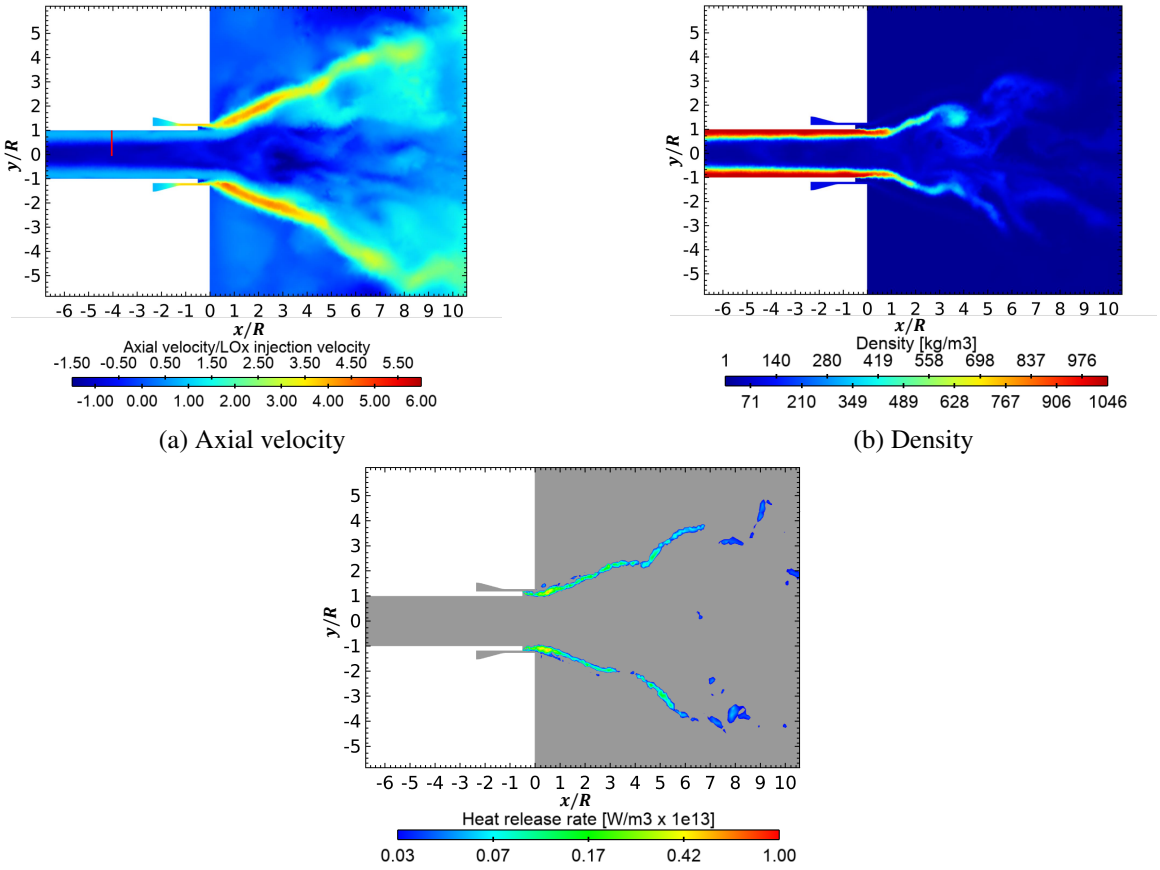

(a) Axial velocity

(b) Density

(c) Heat release rate

Figure 3: Instantaneous flow properties at the the injector exit. R is the LOx tube radius.

and decreases linearly with increasing distance to the wall. Fig. 4d shows that the internal rotational light gaseous core coming from the hot combustor reaches a maximum temperature of 500 K. Therefore, it heats up the LOx film at the interface between the light and dense phases. Then, LOx temperature decreases to a subcritical value near the wall. Consequently, within the swirler, as the distance increases from the wall, LOx gradually evaporates into a gas-like state.

4 Conclusion

The LES of a LOx/CH_4 swirl flame under transcritical conditions is studied for a case ran in the MASCOTTE test bench. Numerical models exhibit a good trend in the initial comparison between experimental and numerical averaged data. Simulations are still running. Models used allow to go further in the investigation of the flame topology, highlighting the presence of a reverse rotational gaseous core within the swirler which destabilizes the LOx film. Also, the flame front is subjected to hydrodynamic instabilities at the injectors exit. Spectral analysis of the density and heat release rate fields are still to be done to explore these instabilities and complete this paper.

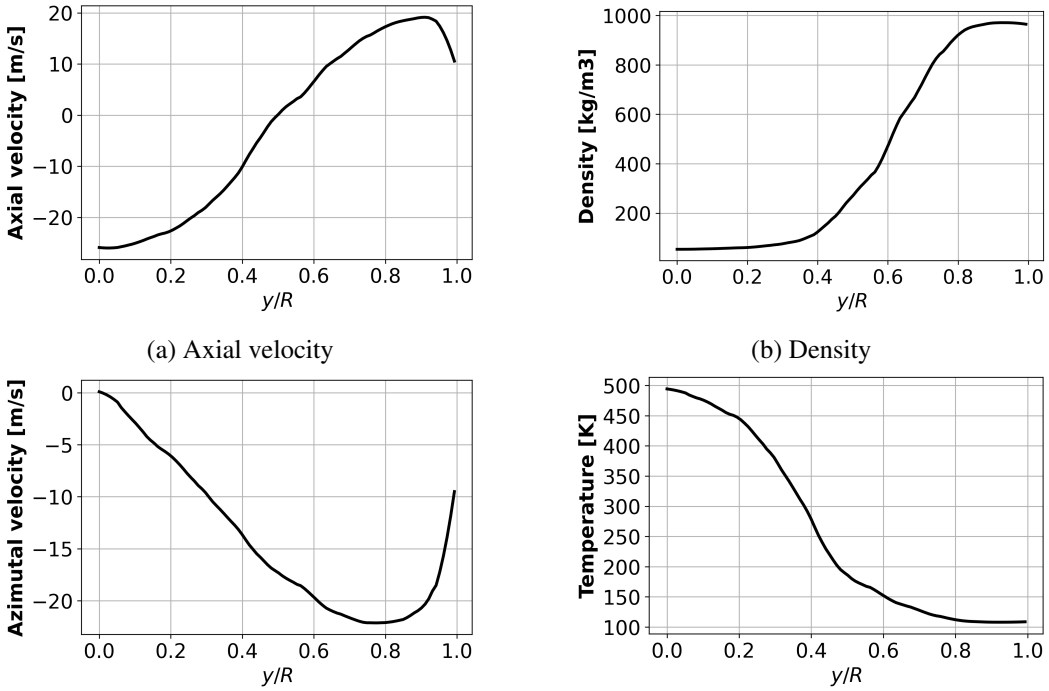

(a) Axial velocity

(b) Density

(c) Azimuthal velocity

(d) Temperature

Figure 4: Radial distributions of time-averaged flow properties at $x/R = -4$. R is the LOx tube radius.

5 Acknowledgments

The authors acknowledge GENCI for providing the computational resources that enabled the realization of these simulations. This work was supported by ONERA and CNES. Authors thank the help of Marie Theron from CNES for supervising this PhD work.

References

[1] Bazarov, V., Yang, V., and Puri, P., *Design and Dynamics of Jet and Swirl Injectors*, chap. 2, Prog. Astronaut. Aero., 2004, pp. 19–103.

[2] Candel, S., Schmitt, T., and Darabiha, N., "Progress in transcritical combustion : experimentation, modeling and simulation," 23rd ICDERS, 2011.

[3] Bouton, M., Nicole, A., Fdida, N., Boulal, S., Vingert, L., Theron, M., Genot, A., and Ribert, G., "Experimental analysis of a LOx/CH4 swirl flame under transcritical conditions," *Combust. Flame*, 2025, ONGOING.

[4] Wang, X., Huo, H., Wang, Y., and Yang, V., "Comprehensive Study of Cryogenic Fluid Dynamics of Swirl Injectors at Supercritical Conditions," *AIAA J.*, Vol. 55, No. 9, 2017.

[5] Zong, N. and Y., V., "Cryogenic fluid jets and mixing layers in transcritical and supercritical environments," *Combust. Sci. Technol.*, Vol. 178, 2006, pp. 193–227.

[6] Wang, X., Li, Y., Wang, Y., and Yang, V., "Near-field flame dynamics of liquid oxygen/kerosene bi-swirl injectors at supercritical conditions," *Combust. Flame*, Vol. 190, 2018.

[7] Sharma, A., De, A., and Kumar, S. S., "Numerical investigation of supercritical combustion dynamics in a multi-element LOx–methane combustor using flamelet-generated manifold approach," *Phys. Fluids*, Vol. 51, 2023, pp. 162–170.

[8] Refloch, A., Courbet, B., Murrone, A., Villedieu, P., Laurent, C., Gilbank, P., Troyes, J., Tessé, L., Chaineray, G., Dargaut, J., Quémerais, E., and Vuillot, F., "CEDRE software," *Aerospace lab*, Vol. 2, 2011.

[9] Nicole, A. and Dorey, L., "REST HF10 test case: Simulation of combustion instabilities induced by flow rate modulations with diffuse interface modelling," 9th EUCASS, Lille, France, 2022.

[10] Bouton, M., Genot, A., Nicole, A., and Ribert, G., "Flame dynamics under methane injection modulations in a transcritical coaxial flow," Space Propulsion, Glasgow, United-Kingdom, 2024.

[11] Boulal, S., Fdida, N., Matuszewski, L., Vingert, L., and Martin-Benito, M., "Flame dynamics of a subscale rocket combustor operating with gaseous methane and gaseous, subcritical or transcritical oxygen," *Combust. Flame*, Vol. 242, 2022.

[12] Chedevergne, F., "Advanced wall model for aerothermodynamics," *Int. J. Heat Fluid Fl.*, Vol. 31, 2010, pp. 916–924.

[13] Rutard, N., Dorey, L.-H., Touze, C. L., and Ducruix, S., "Large-eddy simulation of an air-assisted liquid jet under a high-frequency transverse acoustic forcing," *Inter. J. Multiphas. Flow*, Vol. 122, 2020.

[14] Toro, E., Spruce, M., and Speares, W., "Restoration of the contact surface in the HLLRiemann solver," *Shock waves*, Vol. 4, No. 1, 1994, pp. 25–34.

[15] Saad, Y. and Schultz, H., "A Generalized Minimal Residual Algorithm for Solving Nonsymmetric Linear Systems SIAM," *J. Sci. Statist. Comput.*, Vol. 7, 1986, pp. 856–869.

[16] Petit, X., Ribert, G., Lartigue, G., and Domingo, P., "Large-eddy simulation of supercritical fluid injection," *J. Supercrit. Fluid.*, 2013, pp. 61–73.

[17] Schmitt, T., Méry, Y., Boileau, M., and Candel, S., "Large-Eddy Simulation of oxygen/methane flames under transcritical conditions," *P. Combust. Inst.*, Vol. 33, 2011, pp. 1383–1391.

[18] Touze, C. L., Dorey, L.-H., Rutard, N., , and Murone, A., "A compressible two-phase flow framework for Large Eddy Simulations of liquid-propellant rocket engines," *Appl. Math. Model.*, Vol. 84, 2020, pp. 265–286.

[19] Ribert, G., Domingo, P., Petit, X., Vallée, N., and Blaisot, J.-B., *Modelling and simulations of high-pressure practical flows, In AIAA book series: High-Pressure Flows for Propulsion Applications*, chap. 5, ed. J. BELLAN, 2020, pp. 629–676.

[20] Ely, J. and Hanley, H., "Prediction of transport properties. 1. Viscosity of fluids and mixtures," *Ind. Eng. Chem. Fundam.*, Vol. 20, No. 4, 1981, pp. 323–332.

[21] Gaillard, P., *Interfaces diffuses et flames transcritiques LOx/H2*, Ph.D. thesis, Université Pierre et Marie Curie, 2015.

[22] Fiala, T. and Sattelmayer, T., "On the Use of OH* Radiation as a Marker for the Heat Release Rate in High-Pressure Hydrogen-Oxygen Liquid Rocket Combustion," 49th AIAA/ASME/SAE/ASEE Joint Propulsion Conference, 2013.